Research Article

Aromatic hydroxylation is a major metabolic pathway of the mycotoxin zearalenone in vitro

Erika Pfeiffer[1], Andreas Hildebrand[1], Georg Damm[1], Andreas Rapp[2], Benedikt Cramer[3], Hans-Ulrich Humpf[3] and Manfred Metzler[1]

[1] Institute of Applied Biosciences, Karlsruhe Institute of Technology (KIT), Karlsruhe, Germany
[2] Institute of Organic Chemistry, Karlsruhe Institute of Technology (KIT), Karlsruhe, Germany
[3] Institute of Food Chemistry, University of Münster, Münster, Germany

Zearalenone (ZEN) is a common mycotoxin, for which only reductive metabolites have been identified so far. We now report that ZEN is extensively monohydroxylated by microsomes from human liver *in vitro*. Two of the major oxidative metabolites arise through aromatic hydroxylation and are catechols. Their chemical structures have been unambiguously determined by using deuterium-labeled ZEN and by comparison with authentic reference compounds. Moreover, both catechol metabolites of ZEN were substrates of the enzyme catechol-*O*-methyl transferase. One of the monomethyl ethers represented the major metabolite when ZEN was incubated with rat liver slices, thus demonstrating that catechol formation also takes place under *in vivo*-like conditions. Out of ten major human cytochrome P450 (hCYP) isoforms only hCYP1A2 was able to hydroxylate ZEN to its catechols with high activity. Catechol formation represents a novel pathway in the metabolism of ZEN and may be of toxicological relevance.

Keywords: Aromatic hydroxylation / Catechols / Human liver / Microsomes / Zearalenone

Received: December 20, 2008; revised: January 29, 2009; accepted: January 29, 2009

1 Introduction

The macrocyclic resorcylic acid lactone zearalenone (ZEN, Fig. 1) is produced by *Fusarium* species infesting corn and other grains [1–3]. ZEN exhibits low acute toxicity but a pronounced estrogenic activity [4–6]. Reductive metabolites of ZEN are formed in various animal species and also in humans [7–9], in particular α-zearalenol (α-ZEL, Fig. 1) and its stereoisomer β-zearalenol (β-ZEL). α-ZEL has been found to be even more estrogenic than ZEN, and the hormonal activity of ZEN and its reductive metabolites is believed to be the culprit of numerous reported fertility problems in farm animals, especially pigs, caused by moldy corn and other animal feed contaminated with ZEN [2–6]. The estrogenicity of ZEN may also account for the increased incidence of hepatocellular adenomas seen in female mice and of pituitary adenomas in both male and female mice in a NTP carcinogenicity study [10].

We have recently reported that NADPH-fortified rat liver microsomes, in addition to generating the reductive metabolites α-ZEL and β-ZEL, give rise to several oxidative metabolites [11]. These novel metabolites were tentatively identified as monohydroxylated ZENs, but their complete chemical structures have not yet been elucidated [11]. We have now studied the oxidative metabolism of ZEN and α-ZEL using human hepatic microsomes and recombinant human cytochrome P450 (hCYP) isoforms. In these *in vitro* systems, the two major metabolites of both ZEN and α-ZEL were identified as catechols, resulting from hydroxylation of the aromatic ring. The exact structures were unequivocally established by using ZEN specifically labeled with deuterium at defined positions, as well as synthetic reference compounds and the enzyme catechol-*O*-methyl transferase (COMT). One of the aromatic hydroxylation product is also a major ZEN metabolite in rat liver microsomes. Moreover, rat liver slices incubated with ZEN generated significant amounts of methylated catechols of ZEN and α-ZEL, suggesting that the formation of catechols through

Correspondence: Professor Manfred Metzler, Institute of Applied Biosciences, Karlsruhe Institute of Technology (KIT), P.O. Box 6980, D-76128 Karlsruhe, Germany
E-mail: manfred.metzler@chemie.uni-karlsruhe.de
Fax: +49-721-608-7255

Abbreviations: **BSTFA,** *N,O*-bis(trimethylsilyl)trifluoroacetamide; **COMT,** catechol-*O*-methyltransferase; **CYP,** cytochrome P450; **EI,** electron impact; **hCYP,** human CYP; **HSD,** hydroxysteroid dehydrogenase; **MP,** methylation product; **Rt,** retention time; **SAM,** S-adenosyl-L-methionine; ***t*-BME,** *tert*-butyl methyl ether; **TMS,** trimethylsilyl; **ZEL,** zearalenol; **ZEN,** zearalenone

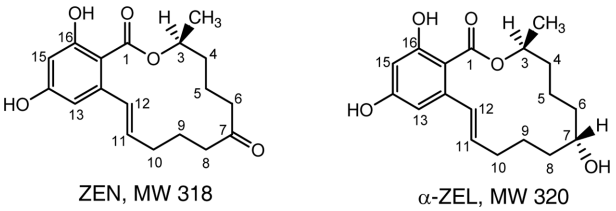

Figure 1. Chemical structures of ZEN and α-ZEL.

aromatic hydroxylation of ZEN also takes place under *in vivo*-like conditions.

2 Materials and methods

2.1 Chemicals

ZEN was purchased from Fermentek (Jerusalem, Israel) and the α- and β-isomers of ZEL from Sigma/Aldrich/Fluka (Taufkirchen, Germany). All compounds had a purity of >98% according to HPLC analysis. Chemicals used for the synthesis of reference compounds, nicotinamide adenine dinucleotide (NAD^+) and its 5′-phosphate ($NADP^+$), S-adenosyl-L-methionine (SAM), *N,O*-bis(trimethylsilyl)trifluoroacetamide (BSTFA), and other chemicals and reagents were of the highest quality available and were also purchased from Sigma/Aldrich/Fluka. HPLC grade ACN was from Acros Organics (Geel, Belgium).

Two types of deuterium-labeled ZEN were used: Dideutero-ZEN, labeled specifically at the two aromatic positions 13 and 15, and hexadeutero-ZEN, labeled at both aromatic positions 13 and 15 as well as at positions 6 and 8 next to the carbonyl group. The 13,15-D_2-ZEN was synthesized by Cramer *et al.* from ZEN-7-[1, 3]dioxolane by alkaline deuterium exchange in deuterated water as reported [12], whereas the 6,6,8,8,13,15-D_6-ZEN was prepared by the same exchange reaction from ZEN in our laboratory according to Miles *et al.* [13]. Analysis by LC-MS in the negative ESI mode gave the following relative intensities of the M-H ions: for D_2-ZEN: *m/z* 319:318:317 = 100:18:8; for D_6-ZEN: *m/z* 323:322:321:320 = 100:68:20:3, indicating a near quantitative exchange of hydrogen.

2.2 Synthesis of reference compounds

2.2.1 13-Nitro-ZEN and 15-nitro-ZEN

100 µL of 65% nitric acid (1 mmol) were added in portions of 20 µL at 5 min intervals to a mixture of 31.8 mg ZEN (100 µmol), 250 µL acetic acid and 100 µL acetic anhydride at 0°C under magnetic stirring. After another 30 min, the orange-colored clear solution was mixed with 2 mL of water and the precipitate extracted into 2 × 3 mL *tert.*-butyl methyl ether (*t*-BME). The combined organic extract was washed with 1 mL of water and dried over $MgSO_4$. According to HPLC-MS analysis, it contained ZEN and two isomers of mononitro-ZEN. These compounds were purified using a Shimadzu CBM-20A preparative HPLC with a 250 × 8 mm i.d, 5 µm, RP Knauer Vertex Eurosphere 100 – C18 column. Solvent A was deionized water adjusted to pH 3.0 with formic acid, and solvent B was ACN. At a flow rate of 4 mL/min and under isocratic conditions of 50% B, a mixture of ZEN and 13-nitro-ZEN eluted after 9 min, whereas pure 15-nitro-ZEN eluted after 12 min. 13-Nitro-ZEN (29 min) and ZEN (31 min) base line-separated when the first fraction was rechromatographed under the following conditions: isocratic at 37% B for 25 min, followed by a linear solvent gradient from 37% B to 50% B in 10 min, then to 100% B in 2 min. After 1 min of eluting the column with 100% B, the initial 37% B were reached in 2 min and kept for 2 min before the next injection. The detector was set to 270 nm. HPLC fractions were concentrated under reduced pressure to remove the ACN, and the pure nitro compounds were extracted from the aqueous solutions with *t*-BME.

13-Nitro-ZEN NMR data ^{1}H NMR (600 MHz, CD_3CN): δ = 1.35 (d, ^3J = 6 Hz, 3 H; 2-CH_3); 1.46 (m, 1 H; H-9); 1.54 (m, 2 H; H-4); 1.71 (m, 2 H; H-5); 2.02 (m, 2 H; H-6 + H-9); 2.11 (m, 1 H; H-10); 2.18 (m, 1 H; H-8); 2.21 (m, 1 H; H-10); 2.31 (br, 1 H; OH-14); 2.61 (dt, ^3J = 12 Hz, ^2J = 4 Hz, 1 H; H-6); 2.78 (ddd, ^3J = 19 Hz, ^3J = 13 Hz, ^2J = 2 Hz, 1 H; H-8); 5.12 (m, 1 H; H-3); 5.52 (ddd, ^3J = 16 Hz, ^3J = 10 Hz, ^3J = 3 Hz, 1 H; H-11); 6.50 (s, 1 H; H-15); 6.69 (d, ^3J = 16 Hz, 1 H; H-12); 11.36 (br, 1 H; OH-16).

^{13}C NMR (125 MHz, CD_3CN): δ = 20.0 (2-CH_3); 20.6 (C-9); 22.2 (C-5); 30.5 (C-10); 34.4 (C-4); 36.2 (C-8); 42.6 (C-6); 74.1 (C-3); 102.8 (C-15); 104.3 (C-16a); 126.3 (C-12); 134.6 (C-11); 135.3 (C-13); 135.8 (C-12a); 153.8 (C-14); 164.6 (C-16); 170.5 (C-1); 210.7 (C-7).

15-Nitro-ZEN NMR data ^{1}H NMR (600 MHz, CD_3CN): δ = 1.38 (d, ^3J = 6 Hz, 3 H; 2-CH_3); 1.61 (m, 2 H; H-4); 1.69 (m, 1 H; H-9); 1.63 – 1.78 (m, 2 H; H-5); 1.91 (m, 1 H; H-9); 2.18 (m, 1 H; H-6); 2.27 (m, 2 H; H-10); 2.36 (m, 1 H; H-8); 2.49 (m, 1 H; H-6); 2.61 (ddd, ^3J = 18 Hz, ^3J = 10 Hz, ^2J = 3 Hz, 1 H; H-8); 5.10 (m, 1 H; H-3); 6.07 (dm, ^3J = 16 Hz, 1 H; H-11); 6.67 (d, ^5J = 4 Hz, 1 H; H-13); 6.82 (d, ^3J = 16 Hz, 1 H; H-12); 9.79 (br, 1 H; OH-14); 12.47 (br, 1 H; OH-16).

^{13}C NMR (125 MHz, CD_3CN): δ = 19.6 (2-CH_3); 20.8 (C-9); 21.6 (C-5); 31.1 (C-10); 34.4 (C-4); 36.4 (C-8); 42.8 (C-6); 74.2 (C-3); 107.0 (C-13); 107.3 (C-16a); 126.3 (C-15); 130.0 (C-12); 137.3 (C-11); 145.7 (C-12a); 154.9 (C-14); 156.6 (C-16); 169.2 (C-1); 210.7 (C-7).

13-Nitro-ZEN GC-MS data (TMS derivative, Rt 25.6 min): 507 (M^+, 22), 490 (17), 472 (49), 460 (78), 442 (18), 430 (10), 416 (14), 400 (51), 382 (25), 378 (33), 360 (26), 348 (40), 340 (37), 324 (100), 308 (65), 290 (29), 288 (30), 276 (20), 260 (25), 250 (35), 235 (23), 216 (8), 169 (17), 151 (11), 125 (12), 73 (29).

15-Nitro-ZEN GC-MS data (TMS derivative, Rt 25.7 min): 507 (M^+, 11), 492 (45), 489 (21), 474 (100), 456

(8), 417 (30), 402 (30), 400 (32), 384 (29), 382 (27), 378 (27), 362 (54), 350 (17), 338 (19), 304 (56), 288 (50), 248 (28), 187 (6), 151 (19), 137 (8), 73 (9).

2.2.2 13-Amino-ZEN and 15-amino-ZEN

At 20°C, a solution of 5.4 mg (15 μmol) of the pure 13-nitro-ZEN or 15-nitro-ZEN in 300 μL of ethanol was added to about 100 μmol of Zn powder activated before by treatment with 1 N aqueous HCl for 10 min followed by exhaustive washing with water and ethanol. 100 μL of formic acid were then added under magnetic stirring. The yellow solution quickly turned colorless. After 30 min, the Zn powder was removed by centrifugation. HPLC-MS and GC-MS analysis showed that the supernatant contains the respective amine in near-quantitative yields without significant byproducts.

13-Amino-ZEN GC-MS data (TMS derivative, Rt 25.2 min): 477 (M^+, 73), 462 (17), 444 (53), 428 (7), 387 (27), 374 (18), 332 (13), 320 (52), 290 (100), 275 (95), 263 (17), 251 (14), 248 (19).

15-Amino-ZEN GC-MS data (TMS derivative, Rt 24.9 min): 477 (M^+, 22), 444 (36), 387 (21), 369 (10), 310 (33), 290 (30), 275 (100), 260 (12), 251 (12), 247 (9).

2.2.3 13-Hydroxy-ZEN and 15-hydroxy-ZEN

The solution of the respective amine (ca. 3.3 mg or 15 μmol) in ethanol/formic acid was concentrated to dryness under a stream of nitrogen, and the residue dissolved in concentrated aqueous ammonia under magnetic stirring at 20°C in the presence of air. Within 5 min, the color of the solution turned from slightly yellow to dark red. The red solution was added to a mixture of 1 mL diluted sulfuric acid (200 μL concentrated H_2SO_4 plus 800 μL water) and 500 μL *t*-BME at 0°C under magnetic stirring. The yellow *t*-BME phase was removed and added to a magnetically stirred solution of 20 mg (95 μmole) of $Na_2S_2O_4 \times 2\ H_2O$ in 1 mL water. After 10 min, the now colorless *t*-BME phase was separated, washed with 200 μL of saturated aqueous NaCl, and dried over $MgSO_4$.

2.3 Cell fractions

Pooled human hepatic microsomes from 24 donors (cat. no. 452161, lot no. 18888, 12 males, and 12 females; 23 Caucasians and 1 Hispanic, with ages ranging from 33 to 78 years) were purchased from BD Gentest (Woburn, MA, USA). Supersomes, *i.e.*, microsomes from insect Sf-9 cells infected with a baculovirus strain containing the cDNA of human CYP1A1, 1A2, 1B1, 2A6, 2B6, 2C8, 2C9, 2C19, 2D6, or 3A4 were also from BD Gentest. 3α-/3β-Hydroxysteroid dehydrogenase (EC 1.1.1.50/51) was purchased from Serva (Heidelberg, Germany). Rat liver cytosol, obtained as the 100 000 × *g* supernatant of the hepatic microsome preparation from male Sprague–Dawley rats as previously reported [11], was used as source of catechol-*O*-methyltransferase (COMT).

2.4 Incubations with CYP isoforms and hepatic microsomes

Individual hCYP isoforms were delivered as suspension in 500 μL buffer with a concentration of 1 nmol CYP per mL. The assays were conducted according to the protocol provided by BD Gentest, taking into account the suitable incubation buffer and incubation time for each isoform to ensure linear kinetics of product formation. In a typical assay with a recombinant hCYP isoform, 2.5 μL of a 10 mM solution of the respective toxin in DMSO and 10 μL of the suspension of the hCYP isoform were added to 500 μL of 0.1 M potassium phosphate buffer pH 7.4 or 0.05 M TRIS/chloride buffer pH 7.5. After 1 min preincubation at 37°C, the enzymatic reaction was started by adding 17.5 μL of a NADPH-generating system, containing 625 μg $NADP^+$, 2.5 μmole $MgCl_2$, 5.2 μmole isocitrate and 0.25 U isocitrate dehydrogenase, and kept at 37°C for the appropriate incubation time. The mixture was then put on ice and extracted twice with 500 μL ethyl acetate each. The combined extract was evaporated to dryness under a stream of nitrogen, and the residue dissolved in 50 μL methanol for HPLC analysis. Control incubations were conducted with microsomes devoid of a hCYP isoform.

Incubation with human hepatic microsomes was carried out in a total volume of 0.2 mL of 0.1 M potassium phosphate buffer pH 7.4 at 37°C for 40 min. The substrate concentration was 100 μM and the microsomal concentration 2 mg protein per mL. The other conditions were the same as used for CYP isoforms.

2.5 Incubations with HSD

Incubations with a mixture of 3α- and 3β-HSD were conducted in a total of 1 mL of 0.1 M potassium phosphate buffer pH 7.4 containing 1 mg HSD (α: 0.05 U/mg; β: 0.03 U/mg) and 3.5 mg NAD^+. About 1 nmol substrate was added as a solution in 10 μL methanol. After 30 min at 37°C, the mixture was cooled on ice and extracted twice with 500 μL ethyl acetate each. Further, work-up was as with microsomal incubations.

2.6 Incubations with COMT

Oxidative metabolites of ZEN or α-ZEL, extracted from the microsomal incubations and fractionated by HPLC (see below), were dissolved in DMSO and added to 250 μL 0.1 M potassium phosphate buffer pH 7.4 containing 4 mM magnesium chloride and 10 μL rat liver cytosol from male Sprague–Dawley rats. The concentration of DMSO in the final incubation did not exceed 1%. After 5 min incubation

at 37°C, 7 µL of a 20 mM solution of SAM in phosphate buffer was added and the incubation continued for another 30 min. Control incubations were run without SAM. The aqueous incubation mixtures were then extracted with ethyl acetate and processed as described for the microsomal incubations.

2.7 Incubations with rat liver slices

Precision-cut slices were prepared from the liver of untreated male Sprague–Dawley rats as previously described [14]. Three liver slices were separately incubated with 200 µM ZEN for 24 h at 37°C in 1.7 mL of Waymouth's medium according to the method of Fisher *et al.* [15]. The incubation media were then separated from the slices and stored at –80°C. For the hydrolysis of glucuronides and sulfates, 200 µL aliquots of the incubation medium were mixed with 200 µL 0.15 M acetate buffer pH 5.0 containing 1000 U of β-glucuronidase type B-1 from bovine liver and 0.1 U of sulfatase type IV from *Acetobacter aerogenes*. Following incubation at 37°C for 2 h, the aglycones were extracted with 2 × 500 µL ethyl acetate. The yield of the extraction procedure was determined with ZEN and α-ZEL, and found to exceed 95% for both compounds. The relative amounts of ZEN and its metabolites were estimated after HPLC analysis from the peak areas, assuming the same extraction yield and absorbance for the metabolites as determined for the parent compound.

2.8 HPLC analysis

For analytical HPLC, a Hewlett Packard 1100 system equipped with a binary pump, a photo-diode array detector and HP ChemStation Rev.A.07.01 software for data collection and analysis was used. Separation was carried out on a 250 × 4.6 mm i.d., 5 µm, RP Luna C18 column (Phenomenex, Torrance, CA, USA). Solvent A was deionized water adjusted to pH 3.0 with formic acid, and solvent B was ACN. A linear solvent gradient was used, changing from 30% B to 70% B in 30 min, then to 100% B in 3 min. After 6 min of eluting the column with 100% B, the initial 30% B were reached in 1 min and kept for 2 min before the next injection. The flow rate was 1 mL/min and the detector was set to 316, 280, and 236 nm. HPLC fractions containing metabolites were collected, extracted with ethyl acetate, and used for GC-MS analysis or for further enzymatic reactions.

2.9 LC-MS/MS analysis

LC-MS experiments were performed using a LXQ Linear IT MSn system (Thermo Fisher Scientific Inc., Waltham, MA, USA) operated in the negative ESI mode. Nitrogen was used as sheath gas and auxiliary gas with flow rates of 30.0 and 15.0 L/min, respectively. Spray voltage was 4.5 kV and capillary temperature was 350°C. Ion optics were automatically tuned with a 10 µM solution of ZEN in methanol. MS/MS of the M-H ions was conducted at CID 35 (35% of 5 kV). The same column and solvents were used as in HPLC but with a different solvent gradient, changing from 30% B to 100% B in 30 min with a flow rate of 0.5 mL/min. For the separation of metabolites peaks 2 and 3, solvent B was kept at 30% for 10 min and then raised to 50% within 15 min.

2.10 GC-MS analysis

A Finnigan GCQ capillary gas chromatograph equipped with a 30 m × 0.25 mm i.d., 0.25 µm, 5% phenylmethyl MDN-5S fused-silica column (Supelco, Bellefonte, PA, USA) and coupled to an IT detector was operated with electron impact (EI) ionization at 70 eV (Thermo Finnigan, Austin, TX, USA). Samples dissolved in methanol or ethyl acetate were evaporated to dryness, dissolved in 20 µL of BSTFA, and 1 µL was injected after a minimum of 3 h, using the splitless mode for 90 s. The injection port temperature was 50°C at the time of injection and, after 30 s, raised to 275°C at 8°C/min. The oven temperature was programmed from 60 (1 min hold) to 290°C (15 min hold) at a rate of 15°C/min. The transfer line and ion source were kept at 275 and 250°C, respectively. Helium was used as carrier gas with a flow rate of 40 cm/s. Mass spectra were scanned from *m/z* 50 to 800 at a rate of 0.5 s/scan.

2.11 NMR spectroscopy

^{1}H- and 2-D NMR data were acquired on a Bruker AVANCE^{TM} 600, ^{13}C-NMR on a Bruker DRX 500 NMR spectrometer (Bruker BioSpin, Rheinstetten, Germany). Signals are reported in ppm referenced to ACN-d_3. For structural elucidation and NMR signal assignment, 2-D NMR experiments, such as 2-D nuclear Overhauser effect spectroscopy (NOESY), correlated spectroscopy (COSY), heteronuclear multiple quantum correlation (HMQC), and heteronuclear multiple bond correlation (HMBC) were carried out. Pulse programs for the experiments were taken from the Bruker software library.

3 Results

3.1 Oxidative metabolites of ZEN and α-ZEL

Human hepatic microsomes were incubated with ZEN in the presence of a NADPH-regenerating system and the incubation subsequently extracted with ethyl acetate. Control incubations without NADPH had shown that more than 95% of the parent mycotoxin were recovered under these conditions. The HPLC profile of the extract from the complete incubation is depicted in Fig.2 (left chart).

The formation of at least seven products was observed which were not generated in the control incubations without

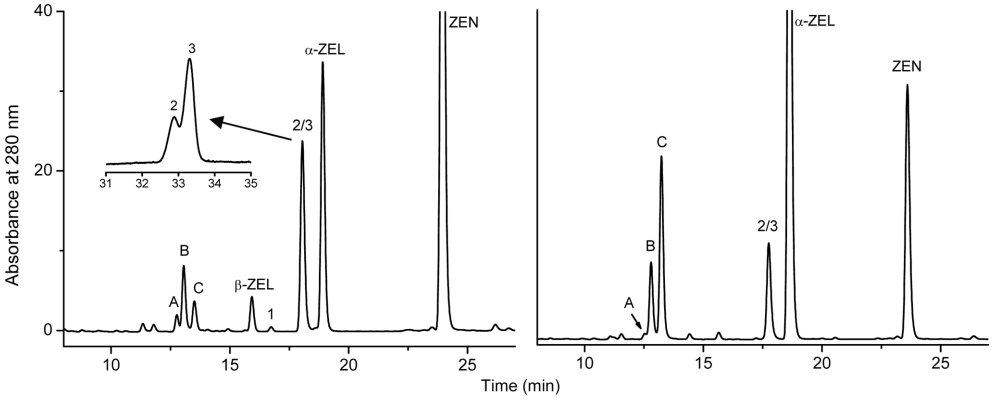

Figure 2. HPLC profiles of the extracts from the incubations of ZEN (left) and α-ZEL (right) with NADPH-fortified human liver microsomes.

NADPH. Two metabolites could be identified as α-ZEL and β-ZEL by co-chromatography with authentic reference compounds in HPLC and, after trimethylsilylation, in GC-MS. Moreover, the ESI and EI mass spectra, obtained by LC-MS and GC-MS, respectively, of the metabolites were identical with that of the reference compounds (Table 1). In LC-MS analysis, HPLC peak 2/3 partly separated into two peaks (Fig. 2, insert in left chart). The mass spectra obtained with ESI in the negative mode suggested that peaks 1–3 were monohydroxylated ZEN (M-H ions at *m/z* 333) and peaks A–C were monohydroxylated ZEL (M-H ions at *m/z* 335); these tentative structures were supported by the EI mass spectra obtained by GC-MS analysis of the respective HPLC peaks after trimethylsilylation (Table 1). The same pattern of metabolites as obtained from ZEN was observed when α-ZEL was incubated with human liver microsomes (Fig. 2, right chart), implying that peaks A–C represented monohydroxylated α-ZEL.

As the position of the newly introduced hydroxyl group could not be deduced from the mass spectra of the ZEN metabolites, two deuterated analogs of ZEN, *i.e.* 13,15-D_2-ZEN and 6,6,8,8,13,15-D_6-ZEN (Fig. 3) were subjected to microsomal metabolism. The same pattern of metabolites was obtained as with unlabeled ZEN. The metabolites were then analyzed by LC-MS/MS employing negative ESI and collision-induced fragmentation of the M-H ions. The daughter ion spectra of HPLC peaks 1–3 and A–C obtained from the unlabeled toxins are depicted in Fig. 4, together with the mass shifts observed for the deuterated compounds. In the spectrum of HPLC peak 1 obtained from D_2-ZEN, the M-H ion and the major fragment ions had a mass increase of 2 amu as compared with the respective metabolite from unlabeled ZEN, indicating that hydroxylation has not occurred at the aromatic ring. The loss of one deuterium, observed for the same metabolite when obtained from D_6-ZEN, suggests that hydroxylation took place at position 6 or 8. Likewise, peak A did not experience deuterium loss when originating from D_2-ZEN but had lost one deuterium when formed from D_6-ZEN. Accordingly, metabolite A is either 6- or 8-hydroxy-α-ZEL. A different result was obtained for HPLC peaks 2 and 3: One deuterium was lost when these metabolites were formed from 13,15-D_2-ZEN, strongly implying that the aromatic ring had been hydroxylated. Likewise, the loss of deuterium observed for HPLC peaks B and C obtained from 13,15-D_2-ZEN suggest that these metabolites arise through aromatic hydroxylation in addition to keto reduction.

Although the use of the deuterium-labeled ZEN provided compelling evidence that the preferred site for the hydroxylation of ZEN and α-ZEL by human hepatic microsomes was position 13 or 15, the data did not allow to differentiate between these sites. Therefore, 13-hydroxy-ZEN and 15-hydroxy-ZEN were chemically synthesized according to the route depicted in Fig. 5. Nitration of ZEN gave rise to a mixture of two mononitro derivatives, which were separated by preparative HPLC and subjected to NMR spectroscopy. For structure elucidation and NMR signal assignment, ^{1}H, ^{13}C, H,H-COSY, H,C-HMQC, H,C-HMBC, and H,H-NOESY spectra were recorded. Analysis of the HMBC and NOESY spectra allowed to unambiguously distinguish the 13-nitro-ZEN and the 15-nitro-ZEN isomer: The NOE spectrum of 15-nitro-ZEN showed a crosspeak between the aromatic proton H-13 and the olefinic proton H-11, whereas the 13-nitro isomer showed no crosspeak between the aromatic and olefinic proton. This structure assignment was supported by the HMBC spectra: Whereas the 15-nitro-ZEN revealed a crosspeak between the olefinic proton H-12 and the aromatic CH-group in position 13, the 13-nitro-ZEN showed a crosspeak between the olefinic proton H-12 and the aromatic C-NO_2.

Subsequent reduction of the pure nitro-ZENs to the respective amino-ZENs, followed by air oxidation to their quinone imines, hydrolysis to quinones, and reduction of the quinones afforded authentic 13-hydroxy-ZEN and 15-hydroxy-ZEN. Whereas 13-hydroxy-ZEN was obtained in near-quantitative yield, the yield of 15-hydroxy-ZEN was only about 10%, possibly due to a higher reactivity of the intermediate quinone imide and/or quinone (Fig. 5). Synthetic 13-hydroxy-ZEN and the ZEN metabolite peak 2 had identical retention time (Rt) in HPLC and (as TMS derivatives) in GC, as well as identical ESI and EI mass spectra (Table 1). Likewise, synthetic 15-hydroxy-ZEN

Table 1. Characterization of ZEN metabolites generated by NADPH-fortified human hepatic microsomes and separated by HPLC

Compound[a]	Rt HPLC (min)	ESI-MS[b] (M-H)	Rt GC[c] (min)	EI-MS[c] m/z (% relative intensity)	Rat liver metabolite[d]	Assigned structure
ZEN	24.0	317	22.2	462 (M^+, 18), 447 (22), 444 (32), 429 (75), 333 (100), 317 (32), 307 (22), 305 (27), 261 (23), 232 (17), 207 (11), 151 (24), 73 (18)	ZEN	ZEN
α-ZEL	19.1	319	22.2	536 (M^+, 13), 446 (100), 431 (51), 413 (26), 361 (27), 333 (39), 307 (39), 305 (36), 73 (28)	M17	α-ZEL
β-ZEL	15.9	319	22.4	536 (M^+, 28), 446 (100), 431 (30), 413 (17), 361 (19), 333 (50), 317 (26), 307 (24), 305 (28), 73 (18)	M14	β-ZEL
peak A	12.8	335	23.7	624 (M^+, 29), 534 (25), 519 (9), 479 (11), 444 (30), 435 (26), 429 (34), 411 (15), 395 (13), 357 (12), 347 (27), 333 (45), 320 (21), 305 (100), 291 (13), 289 (13), 277 (13), 247 (8), 73 (29)	M5	6- or 8-HO-α-ZEL
peak B	13.1	335	22.7	624 (M^+, 8), 609 (42), 534 (29), 519 (100), 501 (23), 465 (22), 449 (20), 429 (94), 421(23), 411 (28), 401 (45), 395 (22), 383 (58), 359 (18), 333 (55), 321 (32), 305 (26), 277 (15), 73 (18)	M6	15-HO-α-ZEL
peak C	13.6	335	23.2	624 (M^+, 100), 609 (75), 534 (56), 519 (94), 501 (35), 468 (19), 449 (22), 444 (38), 421 (37), 395 (43), 383 (39), 379 (14), 305 (12), 291 (13), 277 (9), 225 (8), 203 (6), 73 (18)	M7	13-HO-α-ZEL
peak 1	16.8	333	23.6	550 (M^+, 7), 495 (19), 427 (20), 417 (19), 333 (100), 307 (17), 305 (18), 291 (10), 265 (8), 200 (34), 151 (8), 73 (14)	M15	6- or 8-HO-ZEN
peak 2	18.1[e]	333	23.4	550 (M^+, 38), 535 (33), 517 (100), 442 (18), 421 (26), 405 (24), 395 (30), 363 (71), 348 (83), 317 (40), 151 (23), 73 (18)	n.d.[f]	13-HO-ZEN
peak 3	18.1[g]	333	22.9	550 (M^+, 9), 535 (34), 517 (91), 445 (56), 427 (60), 383 (29), 363 (33), 348 (47), 333 (100), 317 (49), 305 (33), 151 (45), 73 (17)	M16	15-HO-ZEN

a) Designation as in Fig. 2, left chart.
b) Negative mode.
c) After trimethylsilylation.
d) Corresponding metabolite in rat liver microsomes according to ref. [11].
e) Rt LC-MS 32.9 min.
f) n.d., not detected.
g) Rt LC-MS 33.3 min.

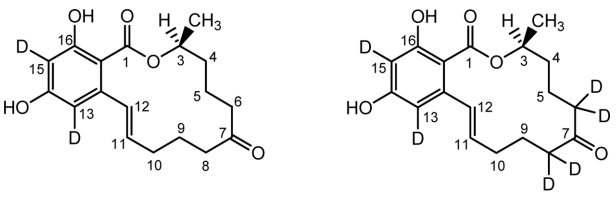

13,15-D_2-ZEN 6,6,8,8,13,15-D_6-ZEN

Figure 3. Chemical structures of deuterated ZEN.

was identical with the ZEN metabolite peak 3 in LC-MS and GC-MS.

The studies using α-ZEL and the deuterium-labeled ZEN described above had shown that HPLC peaks B and C (Fig. 2) are catechol metabolites of α-ZEL. In order to establish their complete chemical structures, peaks B and C were separately collected, extracted from the HPLC fractions, and subjected to enzymatic oxidation using HSD and NAD^+. Previous work from our laboratory [16] has shown that ZEN is obtained from α-ZEL, but not from β-ZEL, indicating a stereoselective oxidation by HSD under these conditions. Metabolite B was converted by HSD/NAD^+ to 15-hydroxy-ZEN with about 50% yield without formation of any 13-hydroxy-ZEN, as shown by GC-MS analysis after trimethylsilylation. Conversely, metabolite C was exclusively oxidized to 13-hydroxy-ZEN with 55% yield. Thus, metabolite B is 15-hydroxy-α-ZEL and metabolite C is 13-hydroxy-α-ZEL (Table 1).

3.2 Methylation of the catechol metabolites of ZEN by COMT

The catechol nature of ZEN metabolites 2 (13-hydroxy-ZEN) and 3 (15-hydroxy-ZEN) was further corroborated by

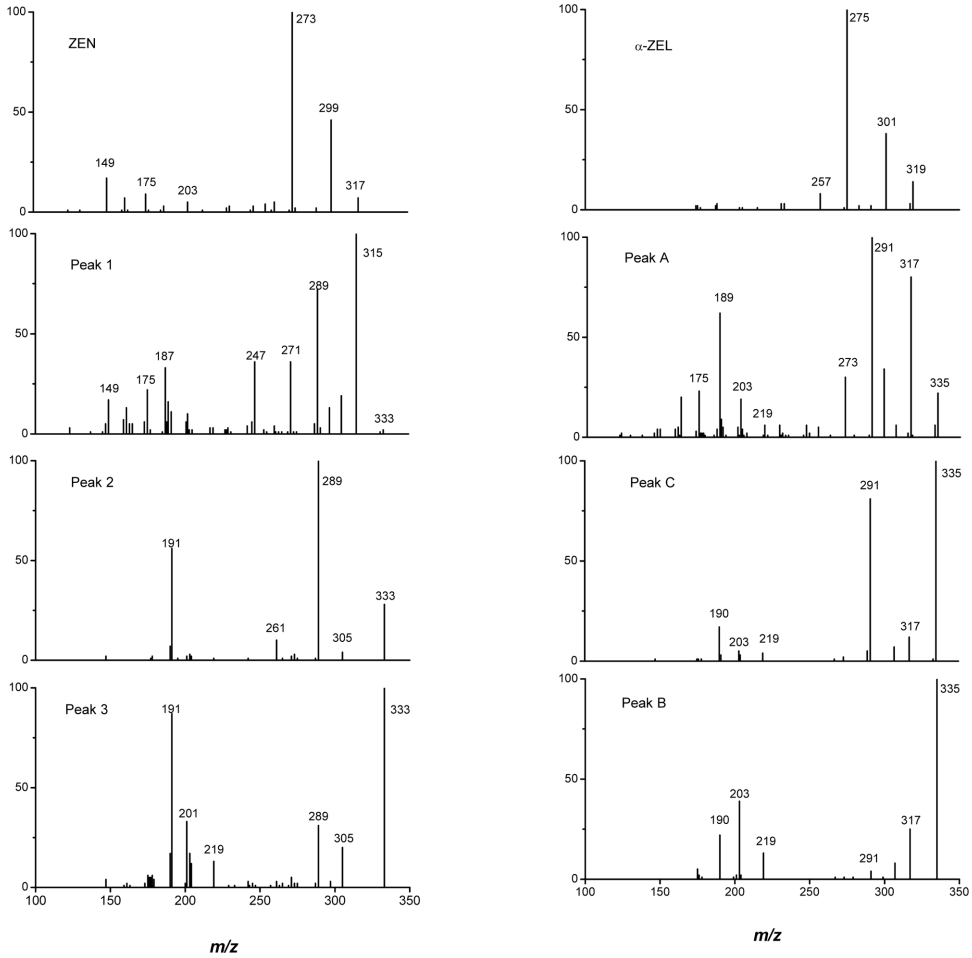

ZEN	175	203	273	299	317
D_2-ZEN	+2	+2	+2	+2	+2
D_6-ZEN	+3	+4	+6	+6	+6
Peak 1	**187**	**247**	**271**	**289**	**333**
D_2-peak 1	+2	+2	+2	+2	+2
D_6-peak 1	+2	+3	+5	+5	+5
Peak 2	**191**	**261**	**289**	**305**	**333**
D_2-peak 2	+1	+1	+1	+1	+1
D_6-peak 2	+2/3		+5	+5	+5
Peak 3	**191**	**219**	**289**	**305**	**333**
D_2-peak 3	+1	+1	+1	+1	+1
D_6-peak 3	+2/3	+3/4	+5	+5	+5

α-ZEL		257	275	301	319
D_2-α-ZEL		+2	+2	+2	+2
D_6-α-ZEN		+6	+6	+6	+6
Peak A	**189**	**219**	**291**	**317**	**335**
D_2-peak A	+2	+2	+2	+2	+2
D_6-peak A	+2	+3	+5	+5	+5
Peak C	**190**	**219**	**291**	**317**	**335**
D_2-peak C	+1	+1	+1	+1	+1
D_6-peak C	+1	+3	+5	+5	+5
Peak B	**190**	**219**	**291**	**317**	**335**
D_2-peak B	+1	+1	+1	+1	+1
D_6-peak B	+1	+3	+5	+5	+5

Figure 4. Daughter ion mass spectra of the M-H ion of ZEN and α-ZEL and their major oxidative metabolites (charts) and shift of ion masses due to the use of D_2- and D_6-labeled ZEN.

the observation that both metabolites are good substrates of the enzyme COMT, which specifically converts catechols to their monomethyl ethers. When ZEN metabolite 2 was purified by HPLC and subsequently incubated with COMT in the presence of SAM, two methylation products (MPs) were obtained at a ratio of about 1 to 9. Both products were monomethyl ethers according to LC-MS and GC-MS, but had different HPLC and GC Rts and mass spectrometric fragmentation (Table 2). Moreover, MP-2 appeared to be chemically stable whereas MP-1 was not. The same MPs were obtained from synthetic 13-hydroxy-ZEN upon incubation with COMT/SAM. Although the exact structures, *i. e.* position of the introduced methyl group, has not yet been determined, it is proposed that MP-1 carries the methyl group at position 14, resulting in a hydroquinone structure which must be expected to autoxidize and there-

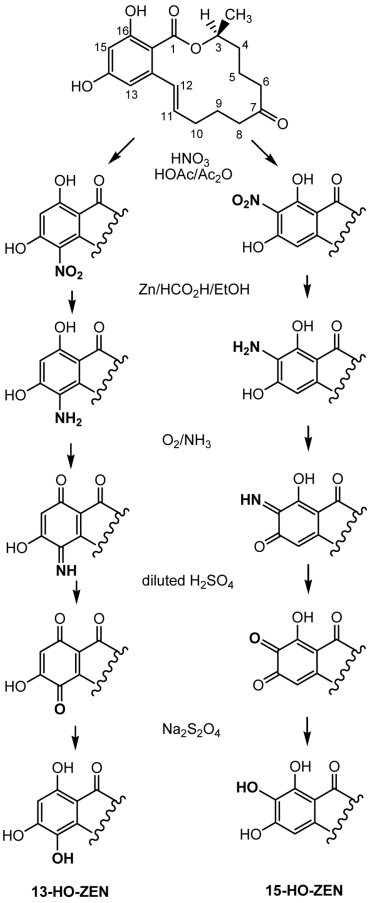

Figure 5. Chemical synthesis of 13-hydroxy-ZEN and 15-hydroxy-ZEN.

fore be unstable; the stable MP-2 of 13-hydroxy-ZEN must then be methylated at position 13, yielding a meta-dihydroxylated aromatic ring which is not susceptible to autoxidation (Fig. 6). Likewise, pure ZEN metabolite 3 as well as synthetic 15-hydroxy-ZEN gave rise to two monomethyl ethers at a 5 to 95 ratio (Table 2). Again, the major product MP-4 was stable whereas the minor MP-3 was not, suggesting that the stable MP-4 carries the methyl group at position 15; the unstable MP-3 is postulated to be methylated at position 14, leaving a catechol structure for autoxidation (Fig. 6). Methylation at position 16 is considered unlikely because this hydroxyl group is engaged in hydrogen bonding with the neighboring carbonyl group. Although the structures of the four MPs are tentative and must await further confirmation, the fact that ZEN metabolites 2 and 3 are substrates of COMT supports their catechol nature.

3.3 Metabolism of ZEN in rat liver slices

The monomethyl ethers of catechol metabolites of endobiotic and xenobiotic compounds are frequently observed as major metabolites *in vivo*. In order to probe whether cate-

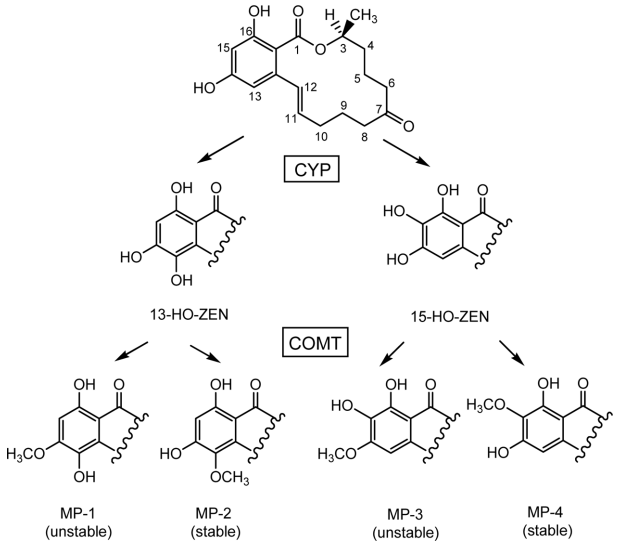

Figure 6. Novel oxidative pathways in the metabolism of ZEN. The assignment of the mono methyl ethers is tentative (see text).

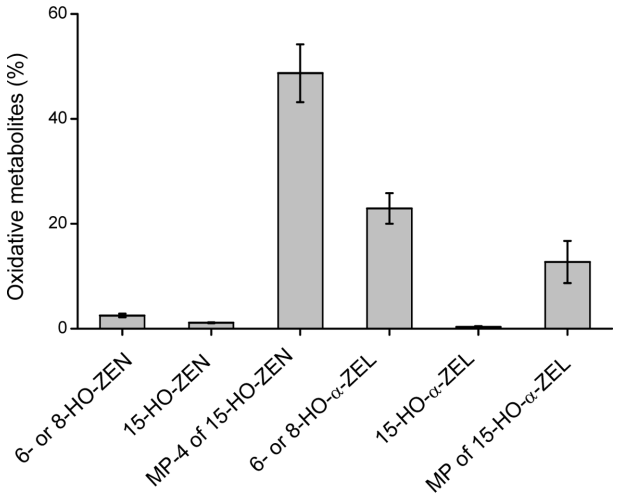

Figure 7. Pattern of oxidative metabolites of ZEN in rat liver slices. Data are the mean ± S.D. of three parallel incubations of slices from the same rat liver.

chol metabolites of ZEN and their monomethyl ethers are formed under *in vivo*-like conditions, *i. e.* in the presence of conjugation reactions, the metabolism of ZEN was studied in precision-cut rat liver slices prepared from male Sprague – Dawley rats. After incubation of three separate slices with 200 μM ZEN for 24 h, the medium was treated with β-glucuronidase and sulfatase for the hydrolysis of conjugates. Aglycones were then extracted and analyzed by HPLC. Approximately 60% of the administered ZEN was recovered as ZEN-related material, consisting of 61.1 ± 2.3% ZEN, 25.5 ± 3.3% α-ZEL and β-ZEL, and a total of 13.3 ± 2.2% hydroxylated metabolites. The pattern of the hydroxylation products is depicted in Fig. 7. LC-MS

Table 2. Characterization of the MP obtained from ZEN metabolites peak 2 (13-hydroxy-ZEN) and peak 3 (15-hydroxy-ZEN) upon incubation with COMT and SAM

Compound		Relative amount (%)	Rt HPLC (min)	ESI-MS[a)] (M-H)	Rt GC[b)] (min)	EI-MS[b)] m/z (% relative intensity)
Peak 2	MP-1	10	23.3	347	22.0	492 (M^+, 46), 477 (39), 474 (22), 459 (100), 428 (9), 384 (15), 369 (35), 363 (39), 354 (16), 347 (13), 337 (21), 335 (19), 331 (15), 321 (14), 305 (28), 290 (27), 275 (26), 266 (12), 260 (13), 151 (25), 73 (4)
	MP-2	90	23.7	347	22.8	492 (M^+, 53), 477 (40), 474 (10), 459 (100), 433 (5), 402 (7), 384 (19), 363 (13), 347 (20), 337 (15), 335 (13), 325 (12), 305 (49), 290 (61), 275 (18), 266 (28), 262 (20), 260 (11), 232 (7), 203 (7), 151 (16), 73 (6)
Peak 3	MP-3	5	22.0	347	23.3	492 (M^+, 27), 477 (24), 459 (100), 415 (6), 402 (6), 384 (16), 363 (9), 347 (12), 337 (14), 335 (10), 325 (17), 305 (26), 290 (40), 275 (26), 266 (19), 263 (11), 247 (12), 233 (8), 209 (9), 151 (17), 73 (6)
	MP-4	95	23.9	347	22.4	492 (M^+, 12), 477 (23), 459 (100), 384 (5), 380 (5), 363 (17), 347 (10), 335 (7), 325 (7), 305 (29), 290 (30), 275 (7), 266 (6), 151 (8), 73 (4)

a) Negative mode.
b) After trimethylsilylation.

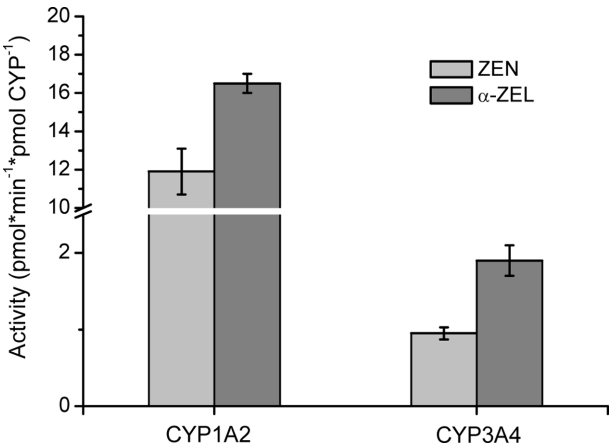

Figure 8. Activities of major hCYP isoforms for the hydroxylation of ZEN and α-ZEL. Data are the mean ± S.D. of three independent experiments.

comparison with the compounds obtained from 15-hydroxy-ZEN through methylation with COMT/SAM (see 3.2) showed that the major metabolite in Fig. 7 was identical with the stable monomethyl ether of 15-hydroxy-ZEN, *i. e.* MP-4 in Table 2 and Fig. 6. A monomethyl ether of 15-hydroxy-α-ZEL was also formed in significant amounts in rat liver slices, together with the products of aliphatic hydroxylation of ZEN and α-ZEL, *i. e.* microsomal metabolites 1 and A (see Fig. 2). Compounds 1 (6- or 8-hydroxy-ZEN) and A (6- or 8-hydroxy-α-ZEL) have also been reported [11] as major ZEN metabolites in rat liver microsomes (Table 1). Only trace amounts of the unmethylated catechol metabolites 15-hydroxy-ZEN (metabolite 3) and 15-hydroxy-α-ZEL (metabolite B) were detected with rat liver slices, which is probably due to their efficient methylation by COMT and their chemical instability. As hydroxylation of ZEN and α-ZEL at C-13 is only a very minor pathway in rat liver microsomes, these catechol metabolites and their monomethyl ethers were not detected in rat liver slices.

3.4 Activity of human CYP isoforms for the hydroxylation of ZEN

In order to clarify which isoforms of hCYP are responsible for the formation of the oxidative metabolites of ZEN and α-ZEL depicted in Fig. 2, the activities of ten major isoforms, *i. e.* 1A1, 1A2, 1B1, 2A6, 2B6, 2C8, 2C9, 2C19, 2D6, and 3A4, for the hydroxylation of the two toxins were determined. As depicted in Fig. 8, hCYP1A2 had by far the highest activity for both ZEN and α-ZEL, and low activity for both toxins was observed for hCYP3A4. α-ZEL but not ZEN was hydroxylated with very low activity by hCYP2D6. The activities of the remaining seven isoforms were below the detection limit of 0.05 pmol × min^{-1} × pmol CYP^{-1}.

GC-MS analysis of the oxidative metabolites of ZEN and α-ZEL generated by hCYP1A2 showed the exclusive formation of the catechol metabolites, *i. e.* 13- and 15-hydroxylation, whereas hCYP3A4 appeared less specific and lead to both aromatic and aliphatic hydroxylation. No reductive or oxidative metabolism at C-7 was noted, probably due to

the lack of steroid dehydrogenases in microsomes from insect cells.

4 Discussion

Until recently, only reductive metabolites of the mycotoxin ZEN have been reported in the literature, in particular α-ZEL and β-ZEL [7 – 9]. In 2007, a study conducted in our laboratory has shown that NADPH-fortified rat liver microsomes give rise to the formation of two major and several minor monohydroxylated ZENs, in addition to α- and β-ZEL [11]. Based on the fragmentation pattern observed in the EI mass spectra after trimethylsilylation, the major oxidative ZEN metabolites were thought to represent hydroxylation products of the aliphatic macrocyclic ring [11]. As shown in the present study, these metabolites were also formed in human hepatic microsomes, together with a third monohydroxylated ZEN not observed in the earlier rat study. However, the use of deuterium-labeled ZEN in the present study clearly established that only one of the major rat metabolites is the product of aliphatic hydroxylation, *i. e.* 6- or 8-hydroxy-ZEN, whereas the other rat metabolite and the novel human metabolite arise from hydroxylation of the aromatic ring. Both products of aromatic hydroxylation of ZEN are catechols. Comparison with authentic reference compounds revealed that the catechol formed by both rat and human hepatic microsomes is 15-hydroxy-ZEN, whereas the second catechol formed only in human microsomes to a significant extent is 13-hydroxy-ZEN (Fig. 6). A recent more detailed analysis showed that 13-hydroxy-ZEN represents only about 5% of the metabolites of ZEN in incubations with rat liver microsomes (Hildebrand, personal communication). The catechol nature of the two major oxidative ZEN metabolites in human hepatic microsomes is supported by methylation with COMT, leading to two monomethyl ethers from each catechol (Fig. 6).

The only clue to catechol formation of ZEN to date has been published by Li *et al*. [17] in a conference proceedings in 1985. A radioenzymatic assay was used, in which catechols generated by microsomal hydroxylation are trapped in a radioactive form by *O*-methylation with COMT, using SAM with a radiolabeled methyl group as the methyl donor. When ZEN was incubated with liver and kidney microsomes of Syrian hamsters under these conditions, a single radioactive peak was observed in HPLC analysis, thought to be the monomethyl ether of a catechol metabolite of ZEN [17]. Similar results were obtained with the α- and β-stereoisomers of ZEL and also of zearalanol, in which the olefinic double bond of ZEL is hydrogenated. However, the radioactive products were not further characterized and the study has not been published in detail.

Whereas our present study unambiguously establishes catechol formation of ZEN as a major metabolic route in human and rat hepatic microsomes *in vitro*, nothing is known about the *in vivo* relevance of this pathway. However, the observed formation of a monomethyl ether of 15-hydroxy-ZEN and of 15-hydroxy-α-ZEL from ZEN in rat liver slices (Fig. 7) clearly demonstrates that hydroxylation of ZEN takes place in the presence of conjugation reactions, strongly suggesting that catechols of ZEN are also formed *in vivo*. As the catechols of ZEN are chemically and metabolically unstable, their concentrations in tissues, blood, and urine must be expected to be low. We therefore propose to use the stable monomethyl ethers of the catechols of ZEN (Fig. 7) or of its major reductive metabolite α-ZEL as biomarkers for catechol formation.

As catechol metabolites of endogenous compounds, *e. g.* 17β-estradiol, and of xenobiotics are often associated with toxic effects such as formation of DNA adducts after further oxidation to quinones or formation of reactive oxygen species through redox cycling [18], the toxicological sequelae of the catechol pathway of ZEN, and related macrocyclic resorcylic acid lactones should now be studied. The reported formation of DNA adducts in the liver and kidney of ZEN-exposed mice, demonstrated by the post-labeling assay, may be associated with the metabolism of ZEN to catechols [19]. Also, the etiology of the tumors observed in the liver and pituitary of mice [10] may not be purely hormonal but involve reactive metabolites of ZEN. It will also be interesting to see whether the catechol metabolites of ZEN and α-ZEL are estrogenic, as they may contribute to the hormonal effects of this mycotoxin. Of particular interest among the congeners of ZEN is α-zearalanol, which is used as a growth promotor in several countries. Using the same approach as described for ZEN in this paper, we have recently shown that α-zearalanol is also prone to catechol formation in liver microsomes from various species [20].

This study was supported by the Deutsche Forschungsgemeinschaft (Grant ME 574/32-1) and by the Research Program "Food and Health" of KIT. We thank Christian Schnattinger for the the preparative HPLC of nitro-ZENs and Doris Honig for helping with the GC-MS analyses.

The authors have declared no conflict of interest.

5 References

[1] European Food Safety Authority, Opinion of the Scientific Panel on Contaminants in the Food Chain on a request from the Commission related to Zearalenone as undesirable substance in animal feed, *EFSA J.* 2004, *89*, 1 – 35.

[2] Kuiper-Goodman, T., Scott, P. M., Watanabe, H., Risk assessment of the mycotoxin zearalenone, *Regul. Toxicol. Pharmacol.* 1987, *7*, 253 – 306.

[3] Bennett, J. W., Klich, M., Mycotoxins, *Clin. Microbiol. Rev.* 2003, *16*, 497 – 516.

[4] Ueno, Y., Tashiro, F. J., α-Zearalenol, a major hepatic metabolite in rats of zearalenone, an estrogenic mycotoxin of Fusarium species, *Biochemistry* 1981, *89*, 563 – 571.

[5] Zinedine, A., Soriano, J. M., Molto, J. C., Manes, J., Review on the toxicity, occurrence, metabolism, detoxification, regulations and intake of zearalenone: an estrogenic mycotoxin, *Food Chem. Toxicol.* 2007, *45*, 1 – 18.

[6] Takemura, H., Shim, J.-Y., Sayama, K., Tsubura, A., *et al*., Characterization of the estrogenic activities of zearalenone and zeranol *in vivo* and *in vitro, J. Steroid Biochem. Mol. Biol.* 2007, *103*, 170 – 177.

[7] Mirocha, C. J., Pathre, S. V., Robison, T. S., Comparative metabolism of zearalenone and transmission into bovine milk, *Food Cosmet. Toxicol.* 1981, *19*, 25 – 30.

[8] Olsen, M., Kiessling, K.-H., Species differences in zearalenone-reducing activity in subcellular fractions of liver from female domestic animals, *Acta Pharmacol. Toxicol.* 1983, *52*, 287 – 291.

[9] Malekinejad, H., Maas-Bakker, R., Fink-Gremmels, J., Species differences in the hepatic biotransformation of zearalenone, *Vet. J.* 2006, *172*, 96 – 102.

[10] National Toxicology Program, *Carcinogenesis bioassay of zearalenone in F344/N rats and B6C3F1 mice.* National Toxicology Program technical report no. 235, 1982. Department of Health and Human Services, Research Triangle Park, NC.

[11] Pfeiffer, E., Heyting, A., Metzler, M., Novel oxidative metabolites of the mycoestrogen zearalenone *in vitro*, *Mol. Nutr. Food Res.* 2007, *51*, 867 – 871.

[12] Cramer, B., Bretz, M., Humpf, H.-U., Stable isotope dilution analysis of the *Fusarium* mycotoxin zearalenone, *J. Agric. Food Chem.* 2007, *55*, 8353 – 8358.

[13] Miles, C. O., Erasmuson, A. F., Wilkins, A. L., Towers, N. R., *et al*., Ovine metabolism of zearalenone to α-zearalanol (zeranol), *J. Agric. Food Chem.* 1996, *44*, 3244 – 3250.

[14] Hoehle, S. I., Pfeiffer, E., Sólyom, A. M., Metzler, M., Metabolism of curcuminoids in tissue slices and subcellular fractions from rat liver, *J. Agric. Food Chem.* 2006, *54*, 756 – 764.

[15] Fisher, R., Smith, P. F., Sipes, I. G., Gandolfi, A. J., *et al*., Toxicity of chlorobenzenes in cultured rat liver slices, *In vitro Toxicol.* 1990, *3*, 181 – 194.

[16] Becker, C., *Nachweis von Zearalenon und Zearalenon-Metaboliten in Fusarien*, Diploma thesis, University of Karlsruhe, 2008.

[17] Li, J. J., Li, S. A., Klicka, J. K., Heller, J. A., Some biological and toxicological studies of various estrogen mycotoxins and phytoestrogens. in: McLachlan, J. A. (Ed.) *Estrogens in the Environment II: Influences on Development*, Elsevier New York, Amsterdam, Oxford 1985, pp. 168 – 181.

[18] Cavalieri, E., Rogan, E., Catechol quinones of estrogens in the initiation of breast, prostate, and other human cancers. Keynote Lecture, *Ann. N. Y. Acad. Sci.* 2006, *1089*, 286 – 301.

[19] Pfohl-Leszkowicz, A., Chekir-Ghedira, L., Bacha, H., Genotoxicity of zearalenone, an estrogenic mycotoxin: DNA adduct formation in female mouse tissue, *Carcinogenesis* 1995, *16*, 2315 – 2320.

[20] Hildebrand, A., Schnattinger, C., Pfeiffer, E., Metzler, M., Catechol formation is a major metabolic pathway of the growth promotor α-zearalanol. *Naunyn-Schmiedeberg's Arch. Pharmacol*. 2009, *379 (Supp. 1)*, 63.

